# Determination of Ice Water Path Over the ARM SGP Using Combined Surface and Satellite Datasets

*J. Huang, M. M. Khaiyer, and P. W. Heck*
*Analytical Services & Materials, Inc.*
*Hampton, Virginia*

*P. Minnis and B. Lin*
*Atmospheric Sciences*
*National Aeronautics and Space Administration*
*Langley Research Center*
*Hampton, Virginia*

*T.-F. Fan*
*Science Applications International Corporation*
*Hampton, Virginia*

## Introduction

Global information of cloud ice water path (IWP) is urgently needed for testing of global climate models (GCMs) and other applications. Accurate quantification of the IWP is essential for characterizing the hydrological and radiation budget. For example, the reflection of shortwave radiation by ice clouds reduces the solar energy reaching the earth's surface. Ice clouds can also trap the longwave radiation emitted from surface, resulting in less radiation to space in comparison with clear-sky conditions. The net radiative flux at surface depends on accurate description of IWP. Determination of cloud IWPs is often complicated because of cloud overlap. Satellite retrievals of IWP are still in the developing stages, and tend to have large uncertainties (e.g., factor of 2 or more).

Ice water path can be inferred from retrievals of cloud optical depth and effective ice particle sizes using visible (VIS) and infrared (IR) methods (e.g., Minnis et al. 1993, 1995) but is greatly overestimated when water clouds are underneath the ice clouds. Methods for direct retrievals of ice cloud properties using millimeter and sub-millimeter-wavelength measurements (Liu and Curry 1998, 1999; Weng and Grody 2000; Zhao and Weng 2002) are under development but have not yet been deployed on satellites. Currently, the most feasible approach for retrieving IWP for the overlapped cases uses a combination of microwave (MW) and VIS/IR methods. Lin and Rossow (1996) estimated global IWP distributions over oceans by using a simple separation technique of total water path (TWP) and cloud liquid water path (LWP) retrieved from VIS/IR data by the International Satellite Cloud and Climatology Project (ISCCP) and a MW remote sensing method, respectively. A more refined microwave, visible, and infrared (MVI) technique (Lin et al. 1998) was used to derive IWP from well-matched VIS IR scanner and Tropical Rainfall Measuring Mission (TRMM) microwave imager data over ocean (Ho et al. 2003). Over land, the variability in surface emissivity renders such an approach nearly useless. However, over the Atmospheric Radiation Measurement (ARM) surface sites, LWP is routinely derived from

microwave radiometers. By combining the geostationary operational environmental satellite (GOES) retrievals with the surface-derived LWP over the ARM site, it is possible to develop an improved IWP climatology over the region.

## Methodology and Data

In this study, the visible infrared solar-infrared split-window technique (VISST) is applied to half-hourly 4-km GOES-8 data during daylight hours (Minnis et al. 2001). For each pixel classified as an ice or water cloud, the VISST derives cloud and radiative properties including IWP or LWP, respectively, for each pixel. The data are processed for a domain centered on the Southern Great Plains (SGP) Central Facility. The value of TWP for a given area is the sum of IWP and LWP derived from GOES-8 using the VISST.

An algorithm adapted from the satellite remote sensing method of Lin et al. (1998, 2001) was used to retrieve LWP and liquid water temperature Tw from the ground-based ARM SGP microwave radiometer (MWR) measurements. ARM's ground-based MWRs are located in several locations within the SGP domain: site B1 located at 38.31°N, 97.30°W (Hillsboro, Oklahoma); B4 at 36.07°N, 99.20°W (Vici, Oklahoma); B5 at 35.69°N, 95.87°W (Morris, Oklahoma); and the Central Facility C1 at 36.61°N, 97.49°W (Lamont, Oklahoma). Cloud base height information was determined using Vaisala ceilometer data at sites B1, B4, and B5 and active remote sensing of cloud layers (ARSCLs; Liljegren 1999; Clothiaux et al. 2000) data at C1. Surface pressure and air temperature, as well as temperature and wind direction at cloud base height, were provided by rapid update cycle 3-hourly model output. The ARM MWRs measure 23.8-GHz and 31.4-GHz brightness temperatures at 20-second sampling intervals. These data were averaged over 3-minute intervals to speed up processing.

The GOES-8 radiances and cloud properties were averaged in 0.3° boxes centered at each site and matched with half-hourly averaged MWR-retrieved cloud properties. Data from March to October 2000 were analyzed to provide an initial daytime climatology of IWP over the SGP sites.

## Results

In this study, the clouds are separated into four groups. Table 1 shows the classification and their occurrence frequency. Here the thermodynamic (ice/water) phases are determined by VISST. The overcast cloud constitutes about 74.2% of the total clouds. Individual overcast clouds of ice, water, and mixed phase occur 18%, 38%, and 18% of the 74.2% total cloud, respectively. Since the MWR provides only one temperature for each 0.3° box and no information about partial cloud coverage, no broken clouds are considered further here. To take into account the advantages of each technique, only those clouds classified as overcast ice phase cloud by VISST will be examined here.

The overcast ice phase clouds actually consist of single-layered ice clouds and ice-over-water cloud. The ice-over-water clouds are identified by the difference between cloud liquid water temperature Tw and the effective cloud temperature Tc. The value of cloud liquid water temperature Tw retrieved from MWR data represents a mean cloud temperature for an integrated cloud column (Lin et al. 1998, 2001)

**Table 1**. Occurrence frequency of clouds classified by GOES-8 during daytime over the ARM SGP domain, March – October 2000

| | Overcast Ice Phase Cloud | Overcast Water Phase cloud | Overcast Mixed Phase Cloud | Broken Cloud | Total |
|---|---|---|---|---|---|
| Number | 863 | 1814 | 887 | 1238 | 4802 |
| Percentage | 16.0% | 37.8% | 18.4% | 25.8% | 100% |

whereas the effective cloud temperature Tc derived from GOES data represents the temperature near the top of the cloud for optically thick clouds (Minnis et al. 1993). When the difference, $\Delta Twc = Tw - Tc$, is significantly positive, it is likely that the observed system consists of overlapped clouds (Lin et al. 1998; Ho et al. 2003). In this study, the condition for classifying a cloud as ice-over-water for the entire 0.3° box is: 100% ice phase, Tc < 273°K, Tw-Tc >8K and MWR LWP >0.0 mm. The ice-over-water clouds are further separated into (a) ice-over-warm-water clouds with optical depth ($\tau$) less than 20; (b) ice-over-warm-water clouds with $\tau$ >20 and ice-over-cold-water clouds (Tw <273 K). Table 2 shows the classification and occurrence frequency of those four cases of ice cloud. Multi-layered clouds were detected in 60% of the total of 863 occurrences of overcast ice clouds for all four sites. Most overlapped cloud systems consist of cold, high ice cloud over lower, warmer water cloud (Figures 1a and b). On average for ice-over-warm-water cloud, Tc from GOES is 52°C less than Tw (Figure 1c), which translates to a height difference of ~7.3 km.

**Table 2**. Classification and occurrence frequency of overcast ice phase cloud over ARM SGP, March-October 2000.

| | Single-Layer Ice Cloud (Tc <273°K, LWP = 0.0) | Ice Over Warm Water Cloud (Tw >≥273°K, $\tau \leq 20$) | Ice Over Warm Water Cloud (Tw >≥273°K, $\tau$ >20) | Ice Over Cold Water Cloud (Tw <273°K) | Total |
|---|---|---|---|---|---|
| Number | 320 | 183 | 311 | 49 | 863 |
| Percentage | 37.1% | 21.2% | 36.0% | 2.7% | 100% |

An analysis of the GOES-8 optical depth for ice-over-warm-water clouds (Figure 2b) yields a mean $\tau$ of $42.3 \pm 35.3$, a value approximately 87% greater than that for the single-layered ice clouds (Figure 2a), indicating a dramatic effect of lower-level water cloud on the derived optical depth. The frequency distributions are also significantly different for those two cloud types. Single-layered ice clouds with $\tau \leq 20$ comprise more than 70% of the total while only 21.2% of the ice-over-warm-water cloud systems have $\tau \leq 20$. Similar results are evident for the ice-over-cold water clouds (Figure 2c).

To further examine the effect of lower-level water clouds on the ice cloud retrievals, the ice-over-warm water cloud systems are separated into two categories based on the GOES optical depth using a threshold of 20. Figure 3 shows the histogram of GOES ice crystal diameter (De) for single-layered ice and ice over warm and cold water clouds. The mean De for single-layered ice clouds (Figure 3a) is around 62 μm, which is about 9% greater than the overall means for the overlapped clouds (Figures 3b

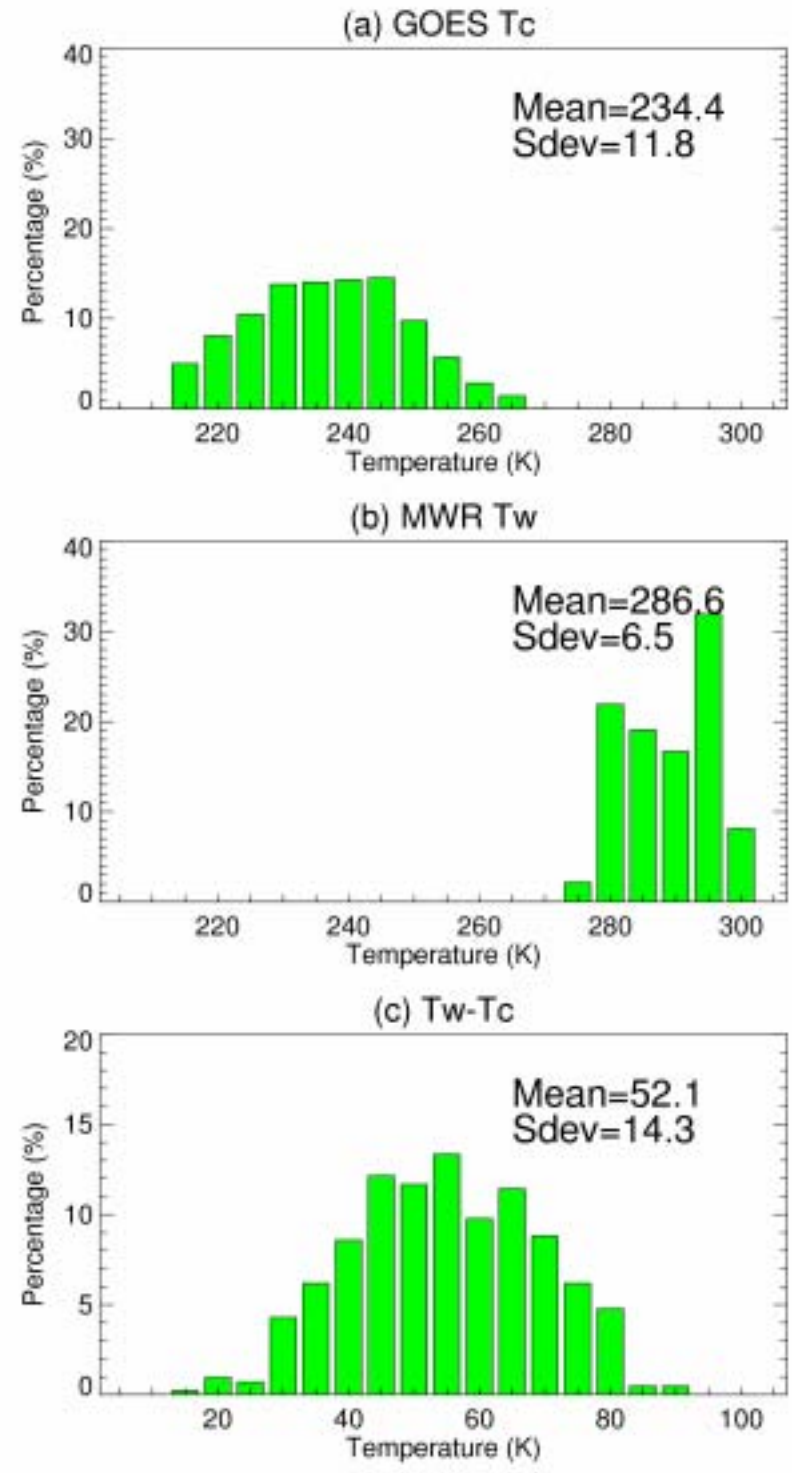


**Figure 1**. Histograms of (a) GOES-8 effective cloud temperature Tc, (b) microwave cloud water temperature Tw, and (c) the difference between Tw and Tc for Ice-over-warm-water clouds over four ARM SGP sites (March-October, 2000).

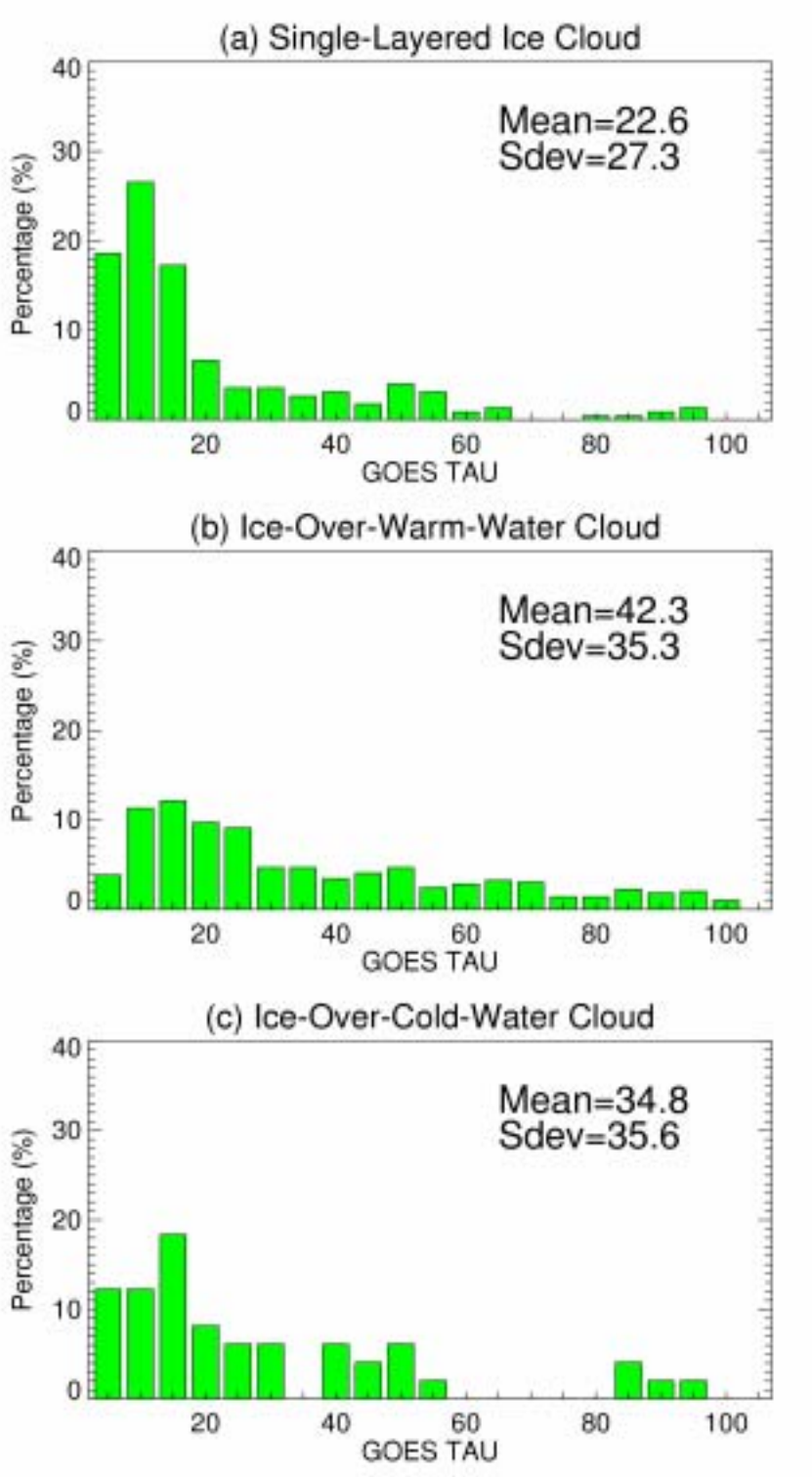


**Figure 2**. Histograms of GOES-8 optical depth for (a) single-layered ice clouds, (b) ice-over-warm-water clouds, and (c) ice-over-cold-water clouds over four ARM SGP sites (March-October, 2000).

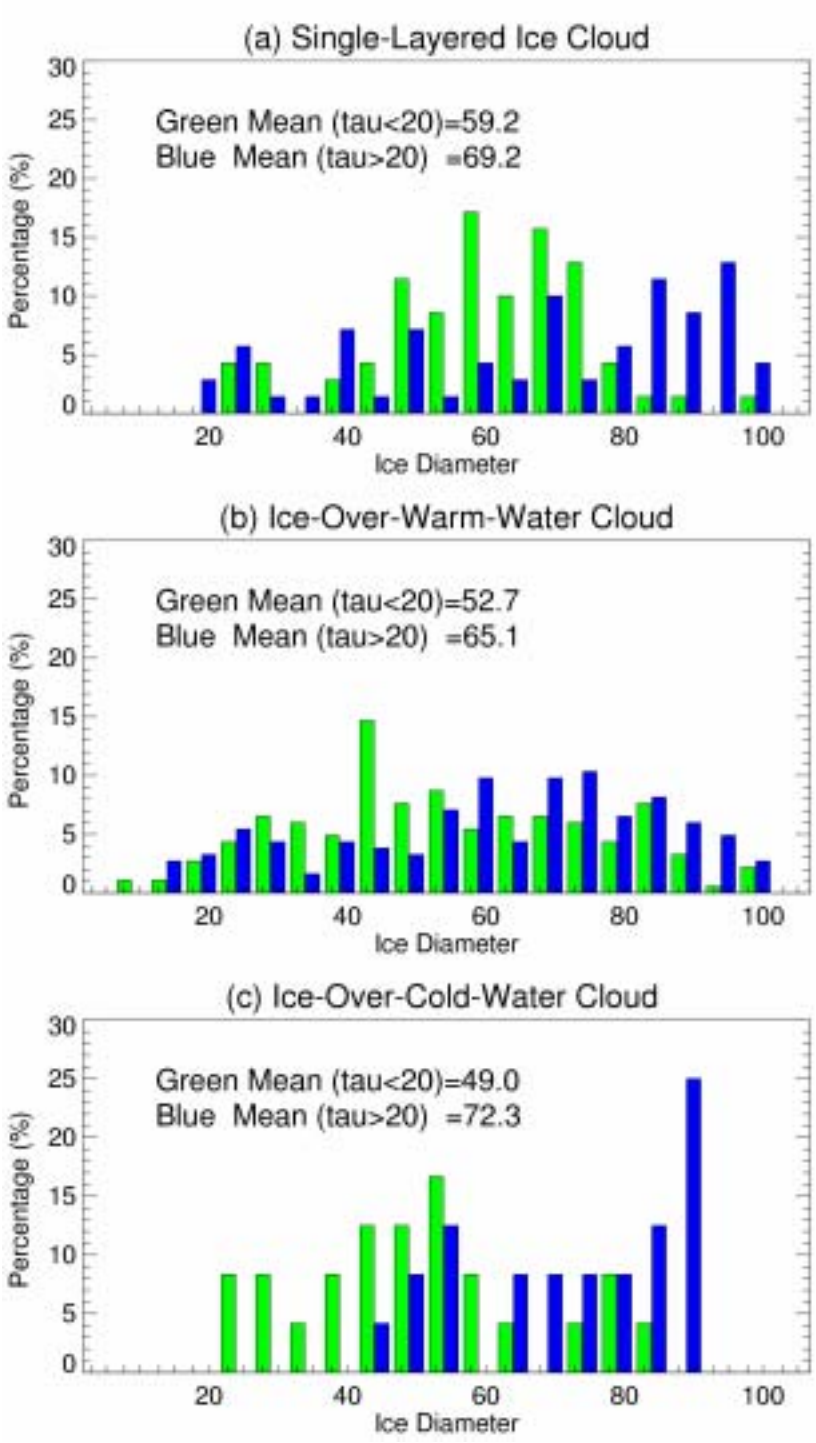


**Figure 3**. Histograms of GOES-8 ice crystal diameter for (a) single-layered ice clouds, (b) ice-over-warm-water clouds, and (c) ice-over-cold-water clouds over four ARM SGP sites (March-October, 2000). The green bar is for tau <20 and blue bar is for tau >20.

and 3c). For single-layered clouds, De is about 10-μm smaller for $\tau \leq 20$ than De for $\tau > 20$. If only the overlapped clouds having $\tau > 20$ are considered then De is much closer to the mean for the single-layered clouds. The average value of De for optically thinner multilayered clouds is 12 - 23 μm smaller than that for the overlapped clouds with $\tau > 20$. The difference could be due to the impact of the underlying water cloud reflectance on the total 3.7-μm radiance used to retrieve De, if the ice cloud is optically thin (Kawamoto et al. 2002). If the optical depth of the ice cloud exceeds 4 or 5, then De should be unaffected by the lower cloud. The similarities in De between the overlapped cases having $\tau > 20$ and the single-layered clouds suggest that there is no distinct difference in De between the single-layered ice cloud and the multilayered clouds.

Figure 4 plots the frequency distributions of GOES TWP, MWR LWP, and MVI IWP (TWP - LWP) for the ice-over-warm-water cloud systems. The green and blue bars represent the overlapped clouds with $\tau \leq 20$ and with $\tau > 20$, respectively. It should be emphasized that the GOES IWP is actually equal to TWP for overcast 100% ice-phase clouds. As shown in Figure 4 for overlapped clouds with $\tau > 20$, the TWP values are considerably larger overall than those for overlapped clouds with $\tau \leq 20$, as expected. For the cases with $\tau \leq 20$, the clouds with MWR LWP less than 0.1 mm account for more than 70% of the total sample, compared to only 36% of those clouds with $\tau > 20$ (Figure 4b). The resulting distributions of IWP in Figure 4c also show a similar difference with 71% of the $\tau > 20$ cases having IWP > 0.2 mm compared to 25% of the retrievals with $\tau \leq 20$. The March-October mean IWP is around 0.92 mm for $\tau > 20$ case, while the averaged IWP is only around 0.09 for $\tau \leq 20$ clouds (Figure 4c). These results suggest that thicker ice clouds are more likely to be coincident with thicker water clouds than with thin water clouds. In Figure 4c, some of the IWP values are negative. Cloud pixels with negative IWP values are mainly due to the uncertainties in the large LWP of lower-level water clouds and some ambiguities in the retrieved IWP when the ice cloud is optically thin. When lower-layer water clouds are drizzling or contain large particles, the VISST may underestimate the LWP for the portion of the overlapped systems (Lin et al. 1998). When the upper-layer cloud is optically thin, the contribution of the ice cloud to the retrieval is relatively small, so that even small errors in the derived LWP can produce negative values. Additionally, differences in the optical properties of water and ice clouds can result in errors in the overall cloud optical depth when only ice is assumed in the VIS retrieval. This can result in errors in TWP. Underestimates in TWP could cause negative values of IWP in some instances.

The daytime variation of hourly mean IWP is shown in Figure 5 for all of the different cloud categories. IWP is at a minimum during early evening for all cloud types, except the ice-over-warm water clouds having $\tau \leq 20$, which have a minimum shortly after noon. Secondary minima occur during the late morning for single-layered and ice-over-cold water clouds. The maximum IWP occurs during the early morning and mid-afternoon for overlapped clouds with ice-over-cold water and with ice over warm water and $\tau > 20$. Single-layered ice clouds peak during mid-morning and mid-afternoon, while the ice-over-warm water clouds with $\tau \leq 20$ have a late morning maximum. For the ice-over-cold-water clouds, the maxima are most likely due to intensifying convection during the afternoon and during the late night because the mean temperature of the water clouds in convective towers should be relatively cold compared to many stratiform cloud systems. The maxima for single-layered ice clouds reflects the persistence of high-level clouds after the nocturnal and afternoon storms dissipate. The variation of the thinner ice-over-warm-water clouds is also probably due to the diurnal cycle in convection. The diurnal

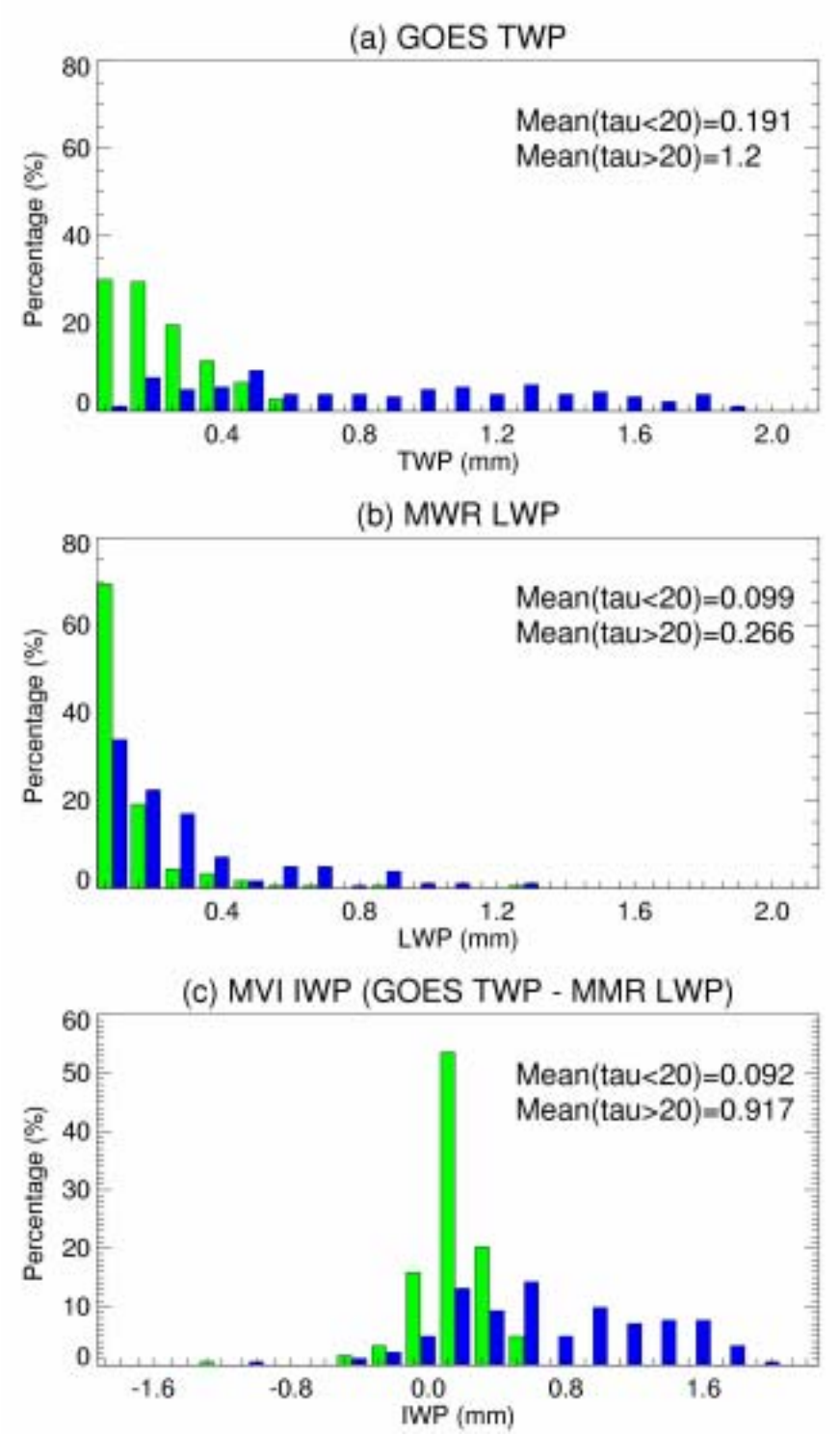


**Figure 4**. Histograms of (a) GOES-8 TWP, (b) MWR LWP, and (c) MVI IWP for ice-over-warm-water clouds over four ARM SGP sites (March-October, 2000). The green bar is for tau <20 and blue bar for tau >20.

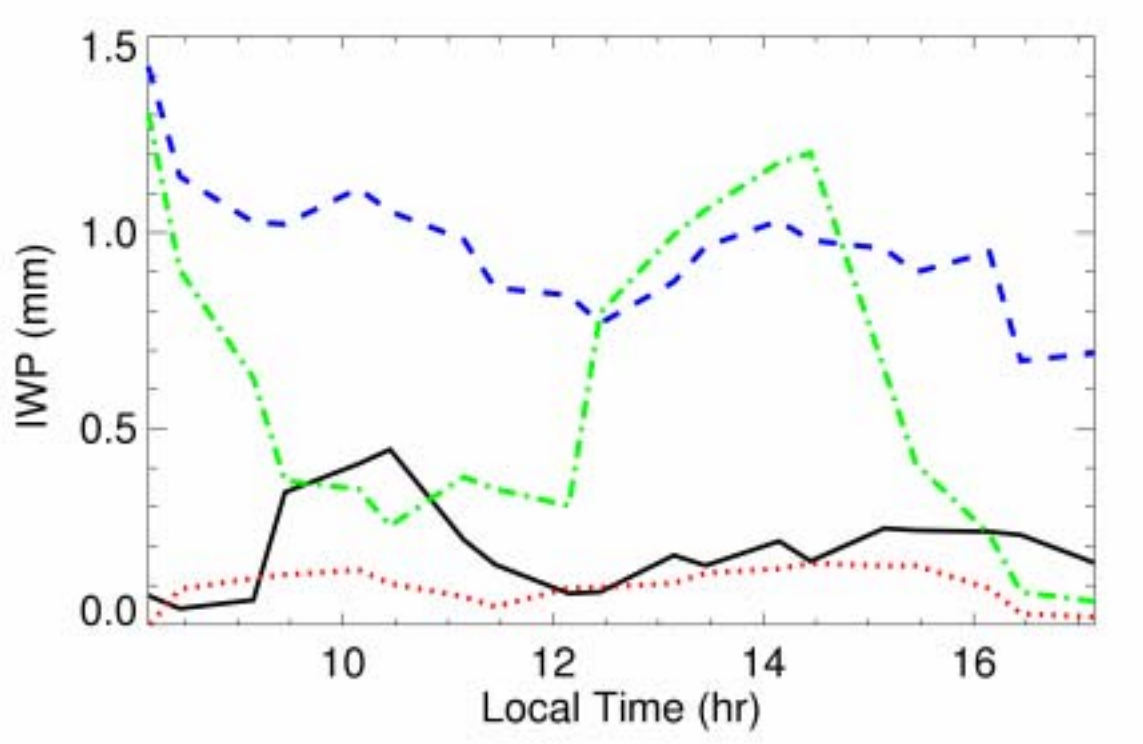


**Figure 5**. Hourly variation of mean IWP of single-layered ice cloud (black line), ice-over-warm-water cloud (tau <20; red line), ice-over-warm-water cloud (tau >20; blue line), and ice-over-cold-water cloud (green line) over four ARM SGP sites (March-October, 2000).

cycle in the thicker ice-over-warm-water clouds is less pronounced and is probably more controlled by synoptic conditions than local surface heating cycles. Figure 5 also shows that the IWP values for thinner ice-over-warm-water clouds are close to those of the single-layered ice clouds. The overlapped systems with $\tau$ >20 most likely contain thicker anvils or convective clouds for the cold water lower clouds and are probably part of baroclinic waves for the warm-water lower clouds.

In reality, the simple differencing of TWP and the MWR LWP may not provide the optimal estimate of IWP because of differences in the scattering properties of liquid and ice clouds because the microphysics of the lower cloud may significantly influence the derived optical depth. To illustrate this point, adding-doubling radiative transfer calculations of VIS (0.65 μm) reflectance were performed using the microphysical model for an ice cloud at a temperature of -40°C (T40; De = 67.6 μm; see Minnis et al. 1998) for various optical depths as a single-layered cloud and as part of a two-layered cloud system. In the latter mode, the underlying cloud was assumed to be composed of water droplets with effective radii of 8 μm (r8) and 12 μm (r12) and the LWP = 0.1 mm. The VIS reflectance was computed for both the single and multi-layered clouds for TWP up to 0.6 mm. Examples of the results are plotted in Figure 6 for two solar zenith $\theta_o$, one viewing zenith $\theta$ (45°), and three relative azimuth $\phi$ angles. In the top panel, the reflectance (red curve) for $\theta_o$ = 60°, $\phi$ = 25° and T40 increases from 0.52 at TWP = 0.1 mm to 0.65 for TWP = 0.2 mm up to 0.84 for TWP = 0.6 mm. The reflectance for T40 at $\theta_o$ = 30° starts at a lower value and follows a similar curve. If a lower-level cloud is inserted, the reflectances increase in all cases for a given TWP. For example, for TWP = 0.1 mm (LWP = 0.1 mm,

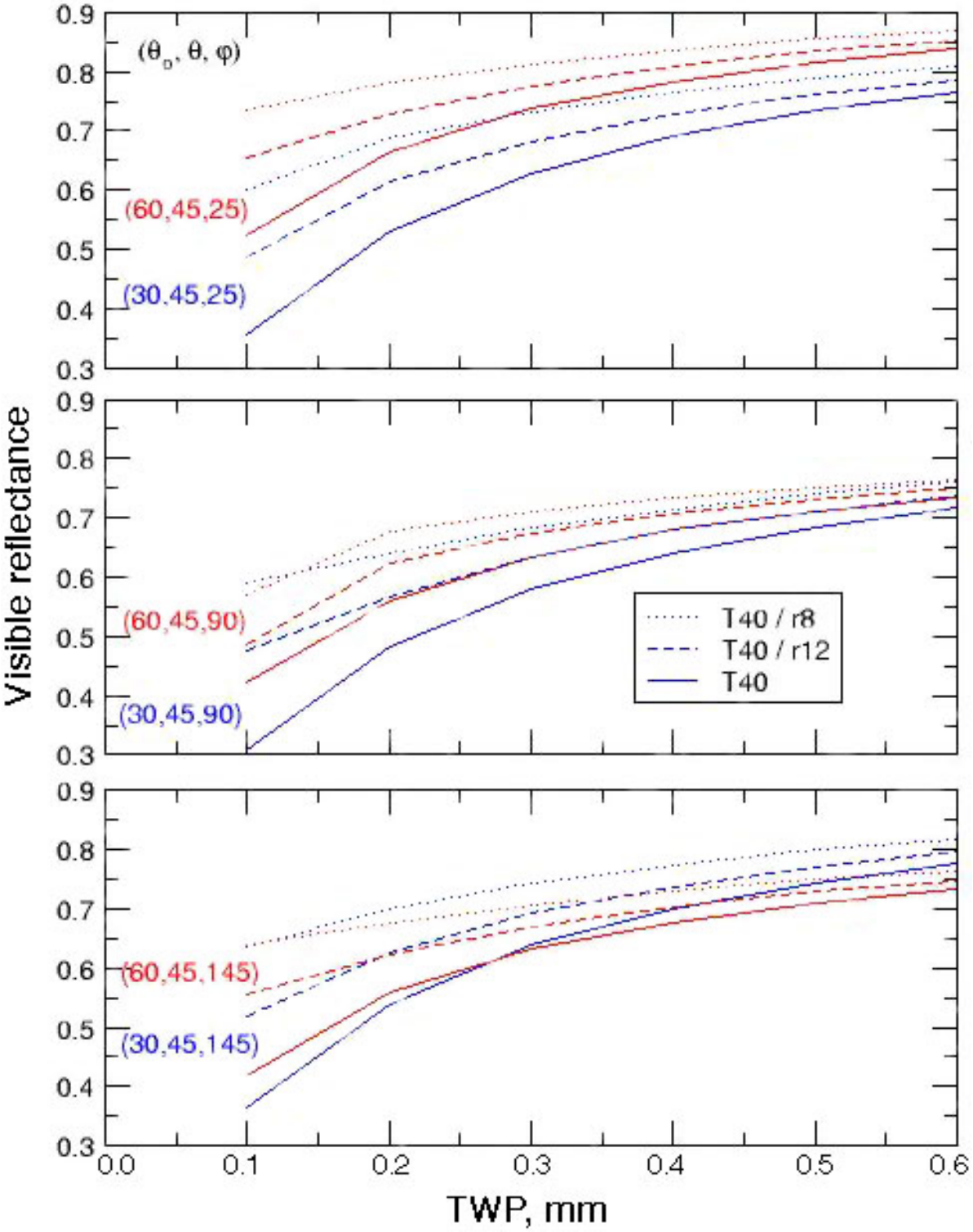


**Figure 6**. Visible reflectance computed for theoretical combinations of single-layered (T40) and two-layered (T40/r8 and T40/r12) clouds.

IWP = 0), T40/r12, and $\theta_o = 60°$, the reflectance is 0.72. If IWP = 0.1 mm (TWP = 0.2 mm), the reflectance is 0.68. If the VISST retrieval assumes the entire cloud is ice, then, following the T40 curve, IWP = TWP = 0.35 mm. If the MWR LWP = 0.1 mm, then the MVI IWP = 0.25 mm instead of the 0.1 mm, a 250% overestimate. The error is even worse for the T40/r8. While the forward scattering direction ($\phi = 25°$) represents an extreme case, most of the other results as seen in the lower panels yield overestimates of IWP from the MVI approach. Thus, the IWP results presented earlier, while likely representative in a relative sense, are biased and are probably much lower than the true values.

## Summary and Future Research

This study has provided the basic framework for estimating IWP in multi-layered cloud systems over the ARM sites using the MVI retrieval algorithm. Distinct differences in the IWP occur for convective, stratiform, and single-layered cloud systems. The MVI differencing approach to deriving IWP in overlapped cases represents a first step toward constructing IWP climatology. Initial analyses of these systems using radiative transfer calculations suggest that differencing approach tends to overestimate IWP. The underlying clouds must be properly characterized and the radiative transfer of the overlapped cloud system must be taken into account. Future research should develop an advanced retrieval method to explicitly account for vertical variations in the cloud layer optical properties that are not taken account with the MVI method. Validation studies of the cloud overlapping and IWP retrievals should be conducted using the ARM cloud radar products. Other efforts to retrieve IWP during the night should also be examined. The combination of different instruments and perspectives unique to the ARM sites should lead to a much improved characterization of ice clouds and their impact on the radiation budget.

## Acknowledgements

This research was supported by the Environmental Sciences Division of U.S. Department of Energy Interagency Agreements DE-AI02-97ER62341 and DE-AI02-02ER63319 under the Atmospheric Radiation Measurement Program.

## Corresponding Author

Jianping Huang, J.Huang@larc.nasa.gov, (757) 827-4624

## References

Clothiaux, E. E., T. P. Ackerman, G. G. Mace, K. P. Moran, R. T. Marchand, M. Miller, and B. E. Martner, 2000: Objective determination of cloud heights and radar reflectivities using a combination of active remote sensors at the ARM CART sites. *J. Appl. Meteorol*., **39**, 645-665.

Ho, S.-P., B. Lin, P. Minnis, and T.-F. Fan, 2003: Estimation of cloud vertical structure and water amount over tropical oceans using VIRS and TMI data. *J. Geophys. Res*., in press.

Kawamoto, K., P. Minnis, W. L. Smith, Jr., and A. D. Rapp, 2002: Detecting multilayer clouds using satellite solar and IR channels. *Proc. 11th AMS Conf. Cloud Physics*., June 3-7, CD-ROM, JP1.18, Ogden, Utah.

Liljegren, J. C., 1999: *Automatic self-calibration of ARM microwave radiometers. Microwave Radiometry and Remote Sensing of the Earth's Surface and Atmosphere*, eds., P. Pampaloni and S. Paloscia, pp. 433-443, VSP Press.

Lin, B., and W. B. Rossow, 1996: Seasonal variation of liquid and IWP in non-precipitating clouds over oceans. *J. Clim*., **9**, 2890-2902.

Lin, B., P. Minnis, B. Wielicki, D. R. Doelling, R. Palikonda, D. F. Young, and T. Uttal, 1998: Estimation of water cloud properties from satellite microwave, infrared and visible measurements in oceanic environments, II: Results. *J. Geophys, Res*., **103**, 3887-3905.

Lin, B., P. Minnis, A. Fan, J. A. Curry, and H. Gerber, 2001: Comparison of cloud liquid water paths derived from in situ and microwave radiometer data taken during the SHEBA/FIREACE. *Geophys. Res. Lett*., **28**, 975-978.

Liu, G., and J. A. Curry, 1998: Remote sensing of ice water characteristics in tropical clouds using aircraft microwave data. *J. Appl. Meteorol*., **37**, 337-355.

Liu, G., and J. A. Curry, 1999: Tropical ice water amount and its relations to other atmospheric hydrological parameters as inferred from satellite data. *J. Appl. Meteorol*., **38**, 1182-1194.

Minnis, P., P. W. Heck, and D. F. Young, 1993: Inference of cirrus cloud properties using satellite-observed visible and infrared radiances, Part II: Verification of theoretical cirrus radiative properties. *J. Atmos. Sci*., **50**, 1305-1322.

Minnis, P., D. P. Kratz, J. A. Coakley, Jr., M. D. King, D. Garber, P. Heck, S. Mayor, D. F. Young, and R. Arduini, 1995: Cloud Optical Property Retrieval (Subsystem 4.3). "Clouds and the Earth's Radiant Energy System (CERES) Algorithm Theoretical Basis Document, Volume III: Cloud Analyses and Radiance Inversions (Subsystem 4)," NASA RP 1376 Vol. 3, ed. by CERES Science Team, pp. 135-176.

Minnis, P., D. P. Garber, D. F. Young, R. F. Arduini, and Y. Takano, 1998: Parameterization of reflectance and effective emittance for satellite remote sensing of cloud properties. *J. Atmos. Sci*., **55**, 3313-3339.

Minnis, P., W. L. Smith, Jr., D. F. Young, L. Nguyen, A. D. Rapp, P. W. Heck, S. Sun-Mack, Q. Trepte, and Y. Chen, 2001: A near-real time method for deriving cloud and radiation properties from satellites for weather and climate studies. *Proc. AMS 11th Conf. Satellite Meteorology and Oceanography*, Madison, WI, Oct. 15-18, 477-480.

Weng, F, and N. C. Grody, 2000: Retrieval of ice cloud parameters using a microwave imaging radiometer. *J. Atmos. Sci*., **57**, 1069-1081.

Zhao, L., and F. Weng, 2002: Retrieval of ice cloud parameters using the advanced microwave sounding unit. *J. Appl. Meteorol*., **41**, 384-395.